

Loci, genes, and mechanisms associated with tolerance to ferrous iron toxicity in rice (*Oryza sativa* L.)

Elsa Matthus¹ · Lin-Bo Wu¹ · Yoshiaki Ueda¹ · Stefanie Höller¹ · Mathias Becker¹ · Michael Frei¹

Received: 22 April 2015 / Accepted: 16 June 2015 / Published online: 8 July 2015
© Springer-Verlag Berlin Heidelberg 2015

Abstract

Key message A genome-wide association study in rice yielded loci and candidate genes associated with tolerance to iron toxicity, and revealed biochemical mechanisms associated with tolerance in contrasting haplotypes.

Abstract Iron toxicity is a major nutrient disorder affecting rice. Therefore, understanding the genetic and physiological mechanisms associated with iron toxicity tolerance is crucial in adaptive breeding and biofortification. We conducted a genome-wide association study (GWAS) by exposing a population of 329 accessions representing all subgroups of rice to ferrous iron stress (1000 ppm, 5 days). Expression patterns and sequence polymorphisms of candidate genes were investigated, and physiological hypotheses related to candidate loci were tested using a subset of contrasting haplotypes. Both iron including and excluding tolerant genotypes were observed, and shoot iron concentrations explained around 15.5 % of the variation in foliar symptom formation. GWAS for seven traits yielded 20 SNP markers

exceeding a significance threshold of $-\log_{10} P > 4.0$, which represented 18 distinct loci. One locus mapped for foliar symptom formation on chromosome 1 contained two putative glutathione-S-transferases, which were strongly expressed under iron stress and showed sequence polymorphisms in complete linkage disequilibrium with the most significant SNP. Contrasting haplotypes for this locus showed significant differences in dehydroascorbate reductase activity, which affected the plants' redox status under iron stress. We conclude that maintaining foliar redox homeostasis under iron stress represented an important tolerance mechanism associated with a locus identified through GWAS.

Introduction

Iron (Fe) toxicity is one of the most commonly observed mineral disorders in rice production affecting millions of hectares of rice land, especially in Southeast Asia and West Africa (Audebert and Fofana 2009; Becker and Asch 2005). It specifically affects rice production, because the low soil redox potential of flooded rice paddies leads to the prevalence of the reduced and soluble Fe^{2+} (ferrous), as opposed to well aerated soils, in which sparingly soluble forms of oxidized Fe^{3+} (ferric) are dominant. Fe toxicity can occur in variable soil types, including acid sulfate or acid clay soils with inherently high Fe concentrations, or poorly drained sandy soils in valleys receiving Fe-rich runoff water from adjacent slopes (Becker and Asch 2005). Fe toxicity causes substantial yield losses in rice and can lead to complete crop failure in severe cases.

Fe is an important plant nutrient and its enrichment in the grain is desirable from a human nutrition perspective (White and Broadley 2009), but foliar tissue concentrations

Communicated by M. Wissuwa.

E. Matthus and L.B. Wu contributed equally to the work.

Electronic supplementary material The online version of this article (doi:10.1007/s00122-015-2569-y) contains supplementary material, which is available to authorized users.

✉ Michael Frei
mfrei@uni-bonn.de

¹ Institute of Crop Science and Resource Conservation (INRES) - Plant Nutrition, University of Bonn, Karlrobert-Kreiten Straße 13, Bonn 53115, Germany

above 300 mg kg⁻¹ are considered as harmful for rice (Dobermann and Fairhurst 2000). Although rice plants possess sophisticated regulatory mechanisms of Fe uptake and homeostasis (Bashir et al. 2010), high amounts of Fe²⁺ in the soil solution can lead to excessive Fe²⁺ uptake and its transport to the shoot via the transpiration stream. Symptoms of Fe toxicity in rice become visible as necrotic brown spots on the leaves termed as ‘leaf bronzing’. These symptoms occur as a consequence of oxidative stress, as Fe²⁺ catalyzes the generation of reactive oxygen species (ROS) via the ‘Fenton reaction’, in which hydrogen peroxide (H₂O₂) oxidizes Fe²⁺ to produce hydroxide (OH⁻) and the highly reactive hydroxyl radical (OH) (Becana et al. 1998). An imbalance of ROS generation in cells and their removal through antioxidants cause irreversible damage of different cellular components such as lipids, proteins, and DNA, and can induce cell death (Blokhina et al. 2003). The hydroxyl radical, which is produced in the presence of Fe²⁺, is considered as the most toxic ROS for plant cells due to the lack of an effective scavenging mechanism through antioxidants (Apel and Hirt 2004).

The breeding of tolerant rice varieties constitutes a powerful approach to address the problem of Fe toxicity. In principle, two physiological strategies may be targeted in achieving this aim: (i) Exclusion of Fe at the root surface by oxidation of Fe²⁺ into insoluble Fe³⁺, which leads to the formation of a root plaque, i.e., precipitates of Fe at the root surface. Root architectural traits favoring this process include the formation of an aerenchyma and a large number of lateral fine roots, which facilitate the diffusion of oxygen into the rhizosphere, thereby increasing the redox potential above the threshold for Fe oxidation (Becker and Asch 2005; Wu et al. 2014). Alternatively, enzymatic Fe oxidation can be catalyzed by enzymes such as peroxidases (Becker and Asch 2005). (ii) Various mechanisms have been proposed conferring ‘shoot tolerance’, i.e., the absence of stress symptoms despite high Fe²⁺ uptake. Fe partitioning both on the organ and the subcellular level may constitute such a mechanism. For example, storage of Fe in the leaf sheaths was proposed to be less damaging than in the photosynthetically more active leaf blades of rice (Engel et al. 2012). On the subcellular level, the vacuole constitutes an important compartment for the storage of excess metal ions (Moore et al. 2014). Much of the plants’ excess Fe is stored in the form of ferritin, a ubiquitous protein occurring in almost all living species, which can store up to 4000 atoms of Fe in a safe and bioavailable form (Arosio et al. 2009; Stein et al. 2009). Another mechanism of shoot tolerance could be the scavenging of ROS through the plants’ antioxidant network, thus avoiding the formation of oxidative stress. However, plants do not possess effective scavengers of the hydroxyl radical—the product of the Fenton reaction (Apel and Hirt 2004). Therefore, antioxidants

would have to remove the precursors of the hydroxyl radical such as hydrogen peroxide, which is reduced to water by antioxidant enzymes such as catalases and peroxidases (Blokhina et al. 2003).

The genetic architecture of tolerance to Fe toxicity in rice appears to be complex. Although quite a few studies reported quantitative trait loci (QTL) for different phenotypes related to Fe toxicity (Dufey et al. 2015; Wu et al. 2014), no major locus has been identified, fine-mapped, or cloned so far. Also, the tolerance rankings of genotypes tested under different natural and artificial environments have sometimes produced contradictory results (Wu et al. 2014), suggesting that the environmental conditions, the timing and level of Fe stress, the screening system, etc., play crucial roles in determining genotype responses to Fe toxicity. Despite these confounding factors, some convergence can be observed on several chromosomal regions, where independent studies reported QTL, including on chromosome 1 between around 25 and 30 Mb and on chromosome 3 between around 0 and 5 Mb (Dufey et al. 2015; Wu et al. 2014). One major limitation of these previous studies was that they all used bi-parental populations, thus covering only a small genetic variability not representing the enormous diversity of Asian rice (*Oryza sativa* L.). Also, the resolution of mapping in these previous studies was limited by a small number of genetic markers (several hundreds) and the typically limited number of chromosomal recombination events occurring in bi-parental crosses (Huang and Han 2014).

To overcome these limitations, we aimed at unraveling genetic and physiological mechanisms underlying tolerance to Fe toxicity by screening a highly diverse population of 329 rice accessions representing the global genetic diversity of rice (Zhao et al. 2011). Screening experiments were followed by a genome-wide association study (GWAS) employing 44,100 single nucleotide polymorphism (SNP) markers to determine candidate loci linked to tolerance. Lastly, one candidate locus, which co-localized with previously reported QTL, was investigated in further detail by sequence and expression analyses of candidate genes and tests of hypotheses related to the physiological mechanism underlying the locus.

Materials and methods

Phenotyping experiment

The population used for genome-wide association study was composed of 329 Asian rice (*Oryza sativa* L.) varieties, originating from 77 countries, covering all major rice-growing regions and five subpopulations of rice, including 74 *indica*, 55 *aus*, 69 *temperate japonica*, 70 *tropical*

japonica, and 12 *aromatic* varieties. Additional 49 accessions were classified as mixed, showing less than 80 % ancestry from any single sub-group. Genotypic data for 44,100 SNPs was publicly available for each line (Zhao et al. 2011). Seeds were obtained from the International Rice Research Institute (IRRI).

Screening experiments were conducted in a hydroponic system (Engel et al. 2012) in the greenhouses of the University of Bonn, Germany, with a 12 h photoperiod, $650 \mu\text{mol m}^{-2} \text{s}^{-1}$ illumination (PAR), and 30/25 °C day/night temperature. Twenty-five seeds per line were germinated in distilled water and then transferred to netted styrofoam trays floating on 0.5 mM CaCl_2 and 10 μM FeCl_3 solution. After 2 weeks, homogenous seedlings of each line were transplanted to 60 L hydroponic containers filled with a modified Yoshida solution (Yoshida et al. 1976), which had the following full strength composition: N 2.86 mM (as NH_4NO_3), P 0.26 mM (as $\text{NaH}_2\text{PO}_4 \times 2\text{H}_2\text{O}$), K 0.82 mM (as K_2SO_4), Ca 0.8 mM (as CaCl_2), Mg 1.3 mM (as $\text{MgSO}_4 \times 7\text{H}_2\text{O}$), Mn 7.3 μM (as $\text{MnCl}_2 \times 4\text{H}_2\text{O}$), Mo 0.4 μM [as $(\text{NH}_4)_6\text{Mo}_7\text{O}_{24} \times 4\text{H}_2\text{O}$], B 14.8 μM (as H_3BO_3), Zn 0.16 μM (as $\text{ZnSO}_4 \times 7\text{H}_2\text{O}$), Cu 0.16 μM (as $\text{CuSO}_4 \times 5\text{H}_2\text{O}$), Fe 28.7 μM (as $\text{FeCl}_3 \times 6\text{H}_2\text{O}$). Plants were fixed with sponges on a perforated lid, and the root of each single plant was separated by a PVC tube fixed underneath the lid to allow each genotype to form its own rhizosphere. To avoid osmotic stress of young seedling, plants were grown in half-strength nutrient solution for the first 10 days. The pH was adjusted to 5.5 twice a week and the solutions were renewed every 10 days.

Until the start of Fe stress, all containers were arranged randomly in the greenhouse to minimize the impact of spatial differences in the microclimate. Each 60 L container contained 40 different and randomly arranged lines. Each experimental cycle included four plants of each genotype in both experimental conditions, of which two were grown in the same planting hole, respectively. This added up to 17 containers for control conditions and 17 containers for the Fe stress treatment. Due to space and labor constraints, but to obtain eight replicate plants per treatment and genotype, two cycles of the experiment described above were carried out from March until June 2013. In summary, eight replicate plants of each line were screened under control conditions and eight replicate plants under Fe stress conditions.

A 5 day Fe pulse stress of 1000 ppm Fe^{2+} (as $\text{FeSO}_4 \times 7\text{H}_2\text{O}$) was imposed 4 weeks after the transplanting. This treatment aimed at simulating acute Fe toxicity during the vegetative growth stage, as it typically occurs in inland valleys during intensive rainfall events (Becker and Asch 2005). To avoid oxidation and precipitation of Fe^{2+} , the solutions were automatically percolated with N_2 gas for 15 min every 2 h. This kept the redox potential below the threshold for iron oxidation (Engel et al. 2012).

As a measure of Fe stress, a leaf bronzing score (LBS) was assigned to the three youngest fully expanded leaves of the main tiller of each plant on day three (LBS3) and day 5 (LBS5) after the application of the stress treatment. The score ranged from 0 (healthy leaf) to 10 (dead leaf) as described by Wu et al. (2014). After 5 days of treatment, all plants were harvested, and the number of tillers, shoot height and root length of each plant were determined. The samples were dried at 70 °C until completely dry and weighed. For Fe concentration analyses, the eight shoot samples from the Fe treatment of each line were pooled and finely ground. A representative sample was analyzed in duplicate by atomic absorption spectrometry as previously described (Wu et al. 2014).

Hypothesis testing experiment

A second experiment was conducted during August/September 2014 to test physiological hypotheses using a subset of lines representing different haplotypes for specific loci. The experimental conditions and experimental systems were identical to those described above. Six hydroponic containers were assigned to three replicate tanks for control and Fe stress treatment, respectively. Each tank contained four replicate plants of each of the eight genotypes tested (single plants per hole). Plant samples were harvested around midday, immediately frozen in liquid nitrogen, and stored at -80 °C for further analysis.

Data analysis and association mapping

Two-way ANOVA tests were applied to analyze the effects of treatment, genotype, and the interaction of both on the phenotypic traits. In both cases, PROC GLM in SAS 9.3 (SAS Institute Inc. Cary, NC) was used and Tukey's HSD test was applied to separate means.

A mean value of the eight replicates of the phenotypic values was used for association mapping. To remove extreme values in each trait, data points which did not fall into the range of (mean of all accessions) \pm (3 times the standard deviation) were removed from the dataset prior to the mapping, which led to the exclusion of a maximum of five values in the case of Fe concentration. To ensure normal distribution of data, square-root transformation was conducted for LBS prior to the mapping, as this trait showed skewed distribution in the original dataset. One-way ANOVA was conducted for subpopulation comparison followed by Tukey's HSD for the post hoc test.

Association mapping was conducted for the whole population and for the subgroups (*japonica* and *indica*) separately, using the software TASSEL 3.0 (Bradbury et al. 2007). SNP marker data, kinship matrix, and principal component analysis (PCA) matrix retaining the four main

axes have been described previously (Zhao et al. 2011). This SNP array provides approximately one SNP marker every 10 kb. SNPs which showed minor allele frequency (MAF) <5 % in our population were removed to avoid overestimation of the effect of SNPs with low frequency. The resultant number of SNPs was 34,564 for the whole panel and 26,621 and 17,106 for the subgroups *indica* and *japonica*, respectively. A mixed linear model (MLM) was used to calculate associations in all analyses, incorporating both PCA and kinship data. The MLM was applied using the default settings (P3D for variance component analysis, compression level set to optimum level). A significance threshold was set to $-\log_{10} P > 4.0$ for in-depth analysis of the most significantly associated markers such as linkage block analysis and curation of candidate gene lists. This threshold was justified by a steep decrease of corresponding q values (Storey and Tibshirani 2003) in the $-\log_{10} P > 4.0$ region and was also applied by other authors using the same population (e.g., Wissuwa et al. 2015). In addition to this significance threshold approach, the 50 most strongly associated markers for each trait were curated as proposed by Verslues et al. (2014) to analyze co-localization of strongly associated markers for different traits, even though they may not exceed a significance value of $-\log_{10} P > 4.0$. Linkage disequilibrium (LD) blocks were defined by the confidence interval method (Gabriel et al. 2002) with default settings using Haploview 4 program (Barrett et al. 2005) based on D' values derived from the SNPs with MAF >5 %. LD blocks harboring significant SNPs were then defined as the candidate loci. The annotations of genes located in these loci were obtained from the MSU7 rice genome database (<http://rice.plantbiology.msu.edu/>, as of October 2014). LD between significant markers and putative functional polymorphisms within candidate genes were assessed by r^2 (Chen et al. 2014) as it takes into account the history of both recombination and mutations (Flint-Garcia et al. 2003).

RNA extraction and quantitative RT-PCR

Shoot samples from the hypothesis testing experiment were immediately frozen in liquid N_2 and stored at $-80^\circ C$. For quantitative real-time polymerase chain reaction (qPCR), mRNA was extracted from three samples per haplotype and treatment using the peqGOLD Plant RNA Kit (Peqlab, Erlangen, Germany). DNA was removed from RNA samples by on-column digestion using a peqGOLD DNase I Digest Kit (Peqlab). RNA concentration was determined using a Nanodrop2000C spectrometer (Thermo Fisher Scientific, Braunschweig, Germany) and the integrity of RNA was checked by denaturing formaldehyde agarose gel electrophoresis. Three hundred ng of total RNA was reverse transcribed with the GoScript™ Reverse Transcription System (Promega,

Mannheim, Germany) and qPCR was performed using the GoTaq® qPCR master mix (Promega) using a StepOne Plus Realtime PCR System (AB Biosystems, Darmstadt, Germany), and the following conditions (Höller et al. 2014): an initial denaturation step (10 min, $95^\circ C$), followed by 40 cycles of denaturation (15 s, $95^\circ C$) and annealing/extension (1 min, $60^\circ C$). Gene-specific primers were as follows: LOC_Os01g49710 forward 5'-CCTGGAGCACTACAA GGGAT-3', reverse 5'-CGAGCAAGGCAGATAGATTG-3'; LOC_Os01g49720 forward 5'-CGTCGTCCTGGAGTA CATC-3', reverse 5'-GACCTGAACAGCACTTTCC-3'. Expression data were quantified using the comparative $\Delta\Delta C_T$ method with the expression level of the sensitive line Guan-Yin-Tsan in the control treatment as calibrator and 18S rRNA as endogenous reference (Frei et al. 2010). Primer efficiency was tested through serial dilutions of cDNA templates and was always above 80 %.

DNA extraction and sequence analyses

Genomic DNA from selected lines was extracted from plant shoots using a PeqGold plant DNA extraction kit (Peqlab). The region of interest was amplified by PCR with the following setup: 25 μL of GoTaq green master mix, 1 μL of each primer (10 μM), 2.5 μL of dimethyl sulfoxide, 15.5 μL of water, and 70 ng of template DNA. The following conditions were used for amplification: $95^\circ C$ for 2 min, 35 cycles of $95^\circ C$ for 30 s, $57/55^\circ C$ for 30 s, and $72^\circ C$ for 2/1.5 min, followed by an additional $72^\circ C$ extension for 5 min. The primer sequences were 5'-CTTTCTGTGATTTGCGATGT-3'/5'-CCGATTCCAACCTTTGCTTA-3' for LOC_Os01g49710 and 5'-GGTGTCTGTAACACTTCCAGTC-3'/5'-AACTTATTCAACCTGCAATCCCTC-3' for LOC_Os01g49720. The amplified DNA was purified after gel electrophoresis using a kit (FastGene Gel/PCR Extraction Kits, Nippon Genetics, Tokyo, Japan). The purified DNA was subjected to a cycle sequencing using the primers used for the PCR. Due to the sequence reading limit, a third primer 5'-GTTCAAGGTGGTGGACGAG-3' was used to complete the sequencing of LOC_Os01g49710. Sequences were compared and analyzed using MEGA 5 software (Tamura et al. 2011). Additional genomic sequences were obtained from the TASUKE rice genome browser (<http://rice50.dna.affrc.go.jp/>) (Kumagai et al. 2013).

Biochemical analyses

Reduced and oxidized ascorbic acid (AsA) was measured in shoots immediately after harvesting (Ueda et al. 2013). Shoot material was ground in liquid nitrogen and about 80 mg of sample material was dissolved in 1 ml 6 % metaphosphoric acid (MPA) containing 1 mM

ethylene-diamine-tetraacetic acid (EDTA). Samples were centrifuged at 15,000g and 4 °C for 20 min. The supernatants were used for further analyses. For the measurements of reduced AsA, 10 µl of the extracts was added to the reaction mix containing 100 mM potassium phosphate buffer (pH 7.0) and 0.1 units of ascorbate oxidase (AO). In the case of oxidized AsA, 10 µl of the extract was added to 100 mM potassium phosphate buffer (pH 7.8) and 4 mM dithiothreitol (DTT). Absorbance was monitored in a microplate reader (Powerwave XSII, BioTek, Bad Reichenhall, Germany) at 265 nm in UV-transparent 96-well microplates until it was constant ($\epsilon = 14.3 \text{ mM}^{-1} \text{ cm}^{-1}$). Total AsA was calculated as the sum of reduced and oxidized AsA.

Glutathione concentration was determined spectrometrically (Griffith 1980). Plant shoots were crushed in liquid *N* and glutathione was extracted from around 100 mg using 1.5 ml of 4 % sulfosalicylic acid and 5 % insoluble polyvinyl-polyrrolidone (PVPP). Samples were centrifuged at 9400g for 10 min at 4 °C, and the supernatant was neutralized by adding 1 M $\text{KH}_2\text{PO}_4/\text{K}_2\text{HPO}_4$. The reaction mix (100 µl) contained 0.6 mM 5,5'-dithiobis-(2-nitrobenzoic acid) (DTNB), 0.2 mM NADPH, and 20 µl of the extract. The reaction was started by adding 0.125 units of glutathione reductase and followed at 412 nm for 3 min. Oxidized glutathione (GSSG) was determined by irreversible derivatization of reduced glutathione (GSH) with 2-vinylpyridine prior to the DTNB reaction.

Enzyme activities were monitored in a microplate reader using 96-well microplates. The activities of ascorbate peroxidase (APX), monodehydroascorbate reductase (MDHAR), and glutathione reductase (GR) were measured using the same plant extract (Frei et al. 2012). Around 100 mg of flash-frozen and ground leaf material was dissolved in 1 ml of 50 mM potassium phosphate buffer (pH 7.8) containing 1 mM AsA and 1 mM EDTA, vortexed, and centrifuged for 30 min at 10,000g and 4 °C. The reaction mix for APX activity (100 µl) contained 100 mM potassium phosphate buffer (pH 6.8), 0.6 mM AsA, 10 µl of 0.03 % H_2O_2 , and 10 µl of enzyme extract. The oxidation of AsA was monitored at 290 nm for 30 s ($\epsilon = 2.8 \text{ mM}^{-1} \text{ cm}^{-1}$).

To determine MDHAR activity, the reaction mix (100 µl) contained 50 mM Tris-HCl buffer (pH 7.6), 0.1 mM NADH, 2.5 mM AsA, 0.1 units ascorbate oxidase, and 10 µl of the plant extract. The oxidation of NADH was monitored at 340 nm for 3 min ($\epsilon = 6.2 \text{ mM}^{-1} \text{ cm}^{-1}$).

GR activity was measured in a reaction mix (100 µl) containing 50 mM potassium phosphate buffer (pH 7.8), 0.12 mM NADPH, 0.5 mM GSSG, and 10 µl of plant extract. Oxidation of NADPH was monitored at 340 nm for 3 min ($\epsilon = 6.2 \text{ mM}^{-1} \text{ cm}^{-1}$).

For determination of dehydroascorbate reductase (DHAR) activity (Hossain and Asada 1984), approximately

100 mg of flash-frozen leaf material was ground and dissolved in 1.5 ml of 50 mM Tris-HCl, 100 mM NaCl, 2 mM EDTA, and 1 mM MgCl_2 . Samples were centrifuged at 13,000g for 5 min at 4 °C. The reaction mix (100 µl) contained 50 mM potassium phosphate buffer (pH 6.5), 0.5 mM dehydroascorbic acid (DHA), 5 mM GSH, and 10 µl of plant extract. Absorbance was followed at 265 nm for 3 min ($\epsilon = 14 \text{ mM}^{-1} \text{ cm}^{-1}$). Protein concentrations in enzyme extracts were determined according to Bradford (1976).

Results

Phenotypic response

Seven phenotypic traits were measured, including biomass and growth-related traits, symptom formation, and Fe concentrations. As we applied an acute stress for a short period of time (5 days) to around 5-week-old plants, biomass-related traits were not strongly affected. On average of all accessions, shoot dry weight was not significantly reduced and root dry weight even increased by around 30 % ($P < 0.001$). Average root length was not affected by the Fe treatment and shoot length slightly decreased by around 4 % ($P < 0.05$). Stress symptoms, as represented by leaf bronzing score (LBS), began to develop after 3 days of Fe treatment and were clearly visible in most accessions 5 days after treatment application. Fe concentrations were measured only in the Fe-treated shoots, since our previous experiments (Engel et al. 2012; Wu et al. 2014) had shown that plants grown under Fe toxicity had shoot Fe concentrations several orders of magnitude higher than in control treatments and therefore do not correlate with values observed under control conditions. Symptom formation (LBS5) and shoot Fe concentration were positively correlated ($-\log_{10} P > 4.0$, Fig. 1a), but the r^2 value indicated that Fe concentrations explained only 15.5 % of the observed variation in leaf bronzing scores. When removing the outlier value with a Fe concentration of 9.2 mg g^{-1} dry weight (Fig. 1a), the r^2 value was even lower (0.1389), but the correlation was still significant ($-\log_{10} P > 4.0$). Tolerant inclusions, i.e., lines with low symptom formation despite high shoot Fe concentration, were represented in all subpopulations of rice (Fig. 1a), indicating that this trait was not specific to any subpopulation. We further compared subpopulation differences for those traits, which we focused on in the association mapping. It was found that *aromatic* and temperate *japonicas* had significantly lower LBS5 and shoot Fe concentrations, suggesting that Fe exclusion was a dominant tolerance mechanism in these subpopulations (Fig. 1b, c). Total Fe uptake was less correlated with symptom formation than Fe concentration and explained

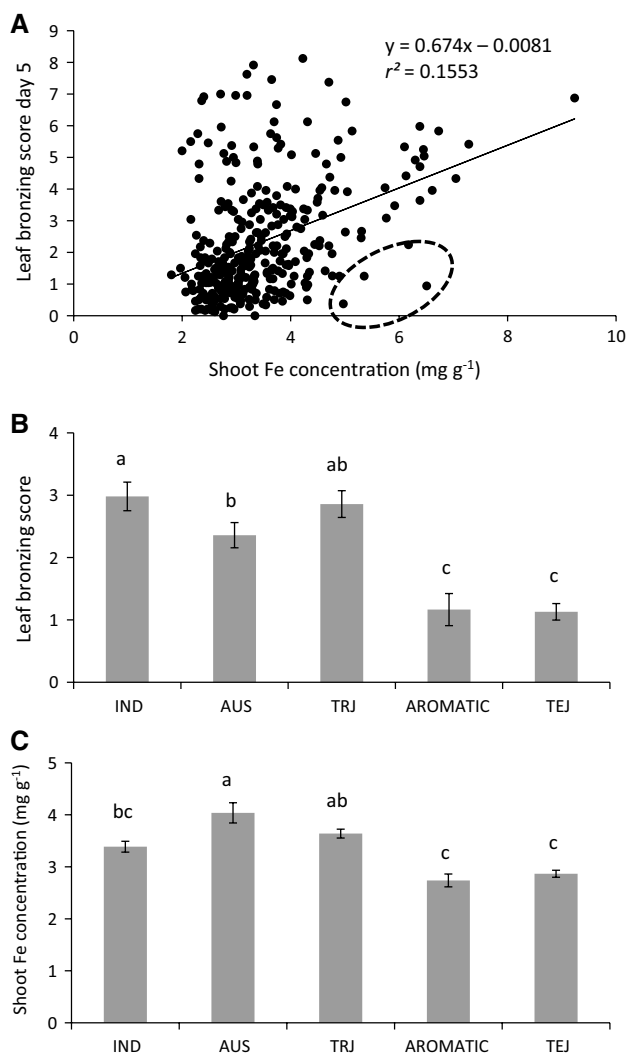


Fig. 1 Analysis of leaf bronzing scores and shoot Fe concentrations in 329 rice lines exposed to Fe toxicity (1000 ppm) for 5 days. **a** Linear regression of shoot Fe concentrations versus leaf bronzing scores. *Encircled data points* represent tolerant inclusions, i.e., accessions with little symptom formation despite high Fe concentration: DM59 (*aus*), Jaya (*indica*), Kamenoo (temperate *japonica*) and Khao Hawm (tropical *japonica*). **b** Sub-population analysis of leaf bronzing score; **c** sub-population analysis of shoot Fe concentrations; *IND* *indica*, *TRJ* tropical *japonica*, *TEJ* temperate *japonica*. *Data bars* show mean values and standard errors; *bars* not sharing the *same letter* are significantly different at $P < 0.05$ by Tukey's HSD test. *Encircled lines* (tolerant inclusions): 322: DM59, Bangladesh, Aus, 76: Jaya, India, Indica, 83: Kamenoo, TEJ, Japan, 89: Khao Hawm, TRJ, Thailand

less than 5 % of the phenotypic variation (Supplementary Figure S1).

Association mapping

Association mapping for all traits included the determination of SNPs exceeding a significance value of $-\log_{10} P > 4.0$, curation of the top 50 most significant SNPs,

analyses of LD blocks surrounding each highly significant ($-\log_{10} P > 4.0$) SNP, and curation of a list of candidate genes contained within these blocks (Supplementary Figures S2–S6, Supplementary Data S7). However, detailed analyses are presented only for those traits which we considered as the most relevant under our experimental conditions, i.e., LBS5 and shoot Fe concentration. Square root-transformed leaf bronzing score (tLBS5) showed nearly normal distribution (Fig. 2a). Mixed model analysis yielded quantile–quantile-plots (q–q plots), which showed upward deviation from the expected $-\log_{10} (P \text{ values})$ only for the most significantly associated markers (Fig. 2b). The significance threshold of $-\log_{10} P > 4.0$ for the association of SNPs with tLBS5 was exceeded in two chromosomal regions (Fig. 2c). On chromosome 1, three highly significant markers were located in two nearby LD blocks (Fig. 2d), which were co-localized with several previously reported QTL (Dufey et al. 2015; Wu et al. 2014). The first block spanned around 82 kb and contained two highly significant SNPs ($-\log_{10} P > 4.0$) and 15 gene models (MSU7), including an FAD binding and arabino-lactone oxidase domains containing protein (LOC_Os01g49360). The second block spanned around 50 kb and contained 14 gene models. The most significant SNP marker (id1016768) was located close to two putative glutathione-S-transferase genes (LOC_Os01g49710, LOC_Os01g49720). We further analyzed phenotypic means of different haplotypes for the three most significant markers on chromosome 1 (Fig. 2e). The most sensitive haplotype TGC only occurred in the *indica* subgroup and was significantly more sensitive than the haplotypes CTA and TGA. These analyses also showed that the A/C SNP id1016768 had the largest effect on the phenotypic means, as the C allele occurred only in the most sensitive haplotype TGC.

A second region on chromosome 5 contained one further SNP exceeding $-\log_{10} P > 4.0$ (id5000074), which was located in a 174 kb LD block. This region did not co-localize with any previously reported QTL (Dufey et al. 2015; Wu et al. 2014). Out of the 36 gene models contained in this linkage block, possible candidate genes related to Fe tolerance included a putative vacuolar ATP synthase (LOC_Os05g01560).

Association mapping for shoot Fe concentration yielded somewhat lower significance values (Fig. 3) with only two SNPs exceeding $-\log_{10} P > 4.0$. The most significant SNP (id2015632) was located within a 12 kb LD block on chromosome 2 (Fig. 3d). This block contained only three gene models, one of which was annotated as a casein kinase I (LOC_Os02g56560). The locus was localized near previously reported QTL for leaf bronzing score and photosynthesis under Fe toxic conditions reported earlier (Dufey et al. 2015; Wu et al. 2014). The second highly significant marker (id1015380) was located outside any LD block on

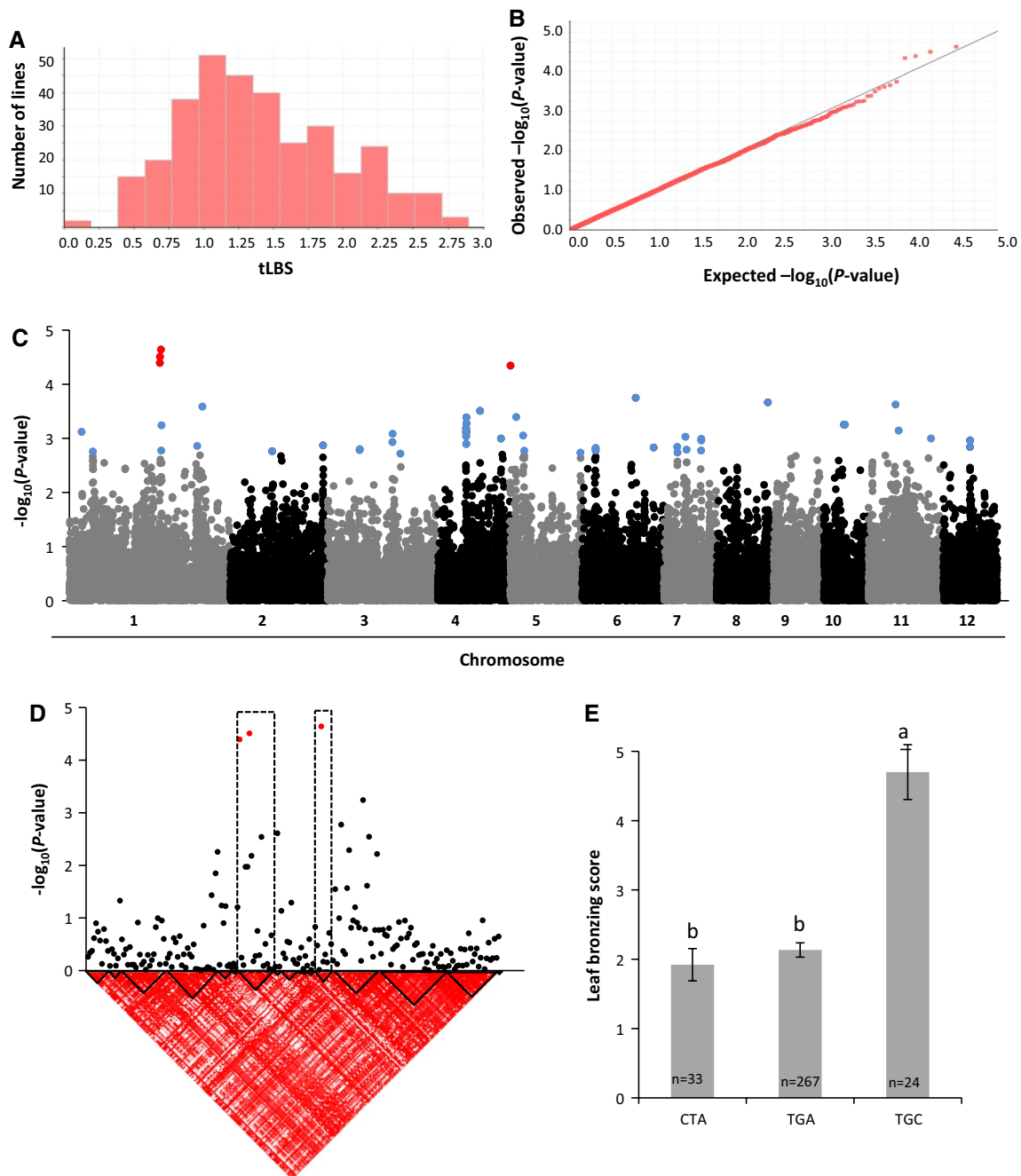


Fig. 2 Association mapping results for square root-transformed leaf bronzing score (tLBS5) after 5 days of Fe treatment. **a** Frequency distribution of tLBS5 in the association panel. **b** q–q plots comparing expected and observed P values for marker–trait associations. **c** Manhattan plot displaying P values for each marker according to mixed linear model analysis. *Blue dots* indicate the top 50 SNPs ($-\log_{10} P$ values ranging from 2.72 to 4.64) and *red dots* indicate SNP exceeding a significance level of $-\log_{10} P > 4.0$. **d** Linkage block analysis

of the candidate locus on chromosome 1; a 1.45 Mb region spanning from 27.85 to 29.30 Mb is shown; *triangles framed in black* indicate linkage blocks determined as stated in “[Materials and methods](#)”. **e** Average leaf bronzing score of contrasting haplotypes for the highly significant ($-\log_{10} P > 4.0$) markers (id1016591, id1016614, and id1016768) on chromosome 1. *Data bars* show mean values and standard errors; *bars not sharing the same letter* are significantly different at $P < 0.05$ by Tukeys HSD test (color figure online)

chromosome 1, but was localized within the broader region (25–30 Mb) on chromosome 1, in which several previously reported QTL are co-localized (Dufey et al. 2015; Wu et al.

2014). Gene models located near the marker and between the two adjacent linkage blocks included a putative potassium ion channel (LOC_Os01g45990).

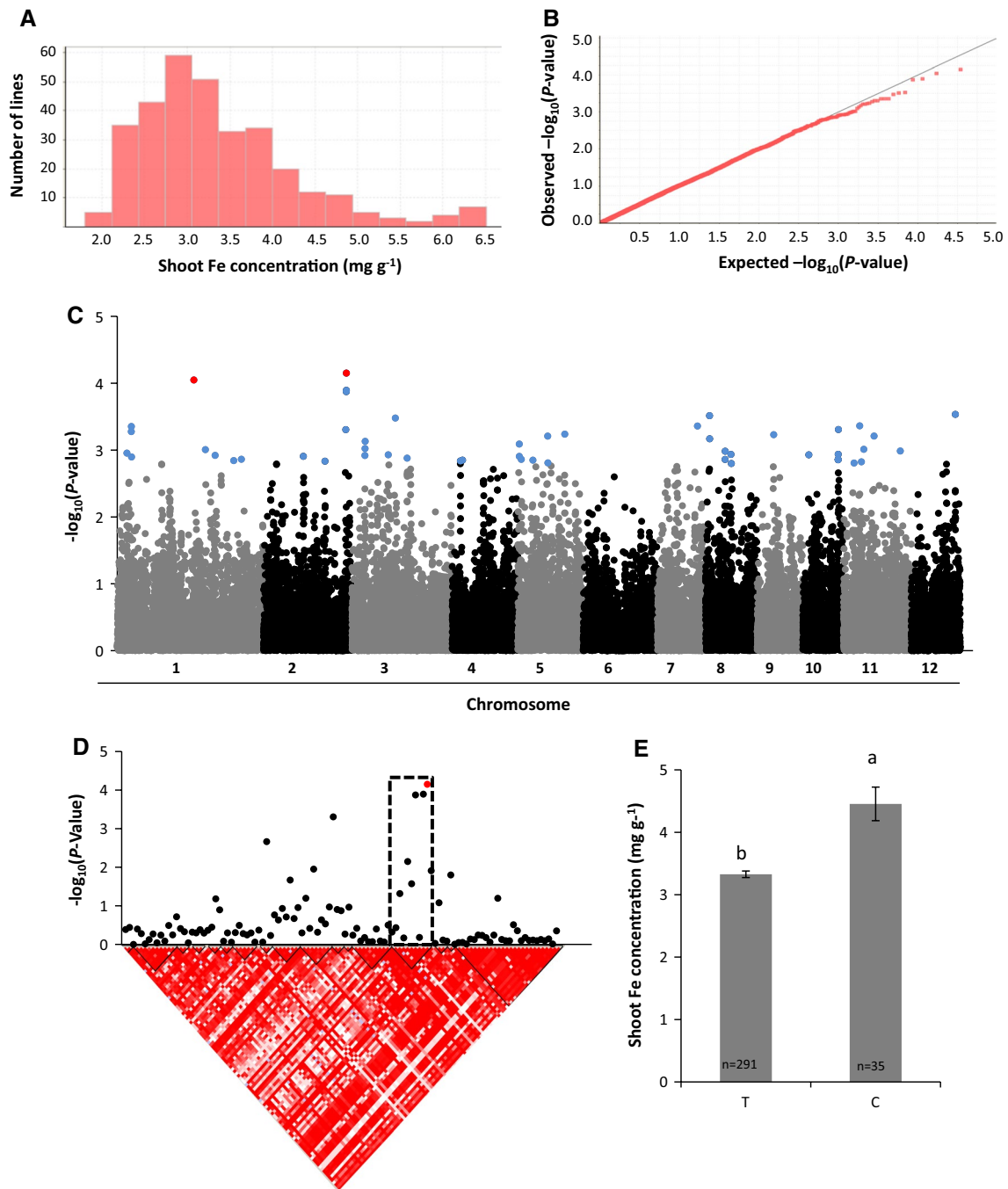


Fig. 3 Association mapping results for shoot Fe concentration after 5 days of Fe treatment (1000 ppm). **a** Frequency distribution of Fe concentrations in the association panel. **b** q–q plots comparing expected and observed P values for marker–trait associations. **c** Manhattan plot displaying P values for each marker according to mixed linear model analysis. *Blue dots* indicate the top 50 SNPs ($-\log_{10} P$ values ranging from 2.80 to 4.15) and *red dots* indicate SNP exceeding the significance level of $-\log_{10} P > 4.0$. **d** Linkage block analysis of the candi-

date locus on chromosome 2; a 0.63 Mb region spanning from 34.21 to 34.84 Mb is shown; *triangles* framed in *black* indicate linkage blocks determined as stated in “Materials and methods”. **e** Average Fe concentrations of lines representing different alleles at the highly significantly ($-\log_{10} P > 4.0$) associated SNP marker (id2015632). *Data bars* show mean values and standard errors; *bars* not sharing the *same letter* are significantly different at $P < 0.05$ by t test (color figure online)

Analysis of candidate locus for tLBS5 on chromosome 1

Among the candidate loci identified through association mapping, we opted to analyze in more detail the locus associated with tLBS5 on chromosome 1 (Fig. 2c–e) as this peak was consistently seen with different mapping approaches: (i) the peak occurred when using a general linear model (GLM, data not shown), as well as the MLM analysis presented here; (ii) the peak also occurred when the MLM was applied to the *indica* subgroup alone (Supplementary Data S7); (iii) for the *indica* subgroup, the most significant markers of this peak (Fig. 2) were also among the top 50 SNPs for tLBS3 (Supplementary Data S7); and (iv) several previous studies with different bi-parental populations had reported QTL for Fe toxicity tolerance in this chromosomal region (Dufey et al. 2015). Eight contrasting *indica* lines were selected to test the hypotheses that (i) Fe toxicity tolerance is related to differential expression or sequence polymorphisms of the candidate genes located in this locus: the glutathione-S-transferase (GST) genes LOC_Os01g49710 and LOC_Os01g49720, and (ii) the locus is associated with differential antioxidant activity. Genomic sequences were analyzed in 30 representative lines. Antioxidants were measured in a sub-set of eight selected lines, four of which represented the sensitive haplotype TGC for the three SNP markers exceeding the significance value of $-\log_{10} P > 4.0$ (Fig. 2), and another four lines represented the tolerant haplotype CTA. These eight lines did not differ significantly in shoot Fe concentration, which was 3.56 mg kg^{-1} on average for the sensitive haplotypes and 3.23 mg kg^{-1} for the tolerant haplotypes, confirming that differences in tolerance occurred due to a shoot-based mechanism rather than Fe exclusion.

Alignment of the genomic sequences of 30 selected lines revealed seven polymorphisms in the gene model LOC_Os01g49710, nine polymorphisms in LOC_Os01g49720, and two polymorphisms upstream of the 5'UTR of LOC_Os01g49720 (Fig. 4a). Five of these polymorphisms were in complete LD ($r^2 = 1$) with the nearby marker id1016768, which had the most significant P value for tLBS5. Among those polymorphisms, one SNP was located upstream of the 5'UTR of LOC_Os01g49720, and one in the coding sequence of LOC_Os01g49720. These SNPs did not change the predicted amino acid sequence of the protein or cause any genotypic difference in mRNA expression (Fig. 4c). In contrast, three insertion deletions (INDELs) in LOC_Os01g49710 were in complete LD ($r^2 = 1$) with the marker id1016768 (Fig. 4a). The sensitive haplotype TGC had an 18-nucleotide insertion (GST1_INDEL50) in the first exon, which added six glycine units to the predicted protein sequence and another 2-nucleotide frameshift deletion (GST1_INDEL734) in the second exon. A third 1-nucleotide insertion was located in the 3'UTR

(GST1_INDEL978). Both candidate genes showed highly significant mRNA up-regulation under Fe stress (Fig. 4b, c), but no significant difference between the haplotypes. In summary, these data demonstrated that both candidate genes were highly responsive to Fe stress and had sequence polymorphisms in complete LD with the most significant SNP marker, which in the case of LOC_Os01g49710 may cause substantial modifications in the protein structure.

Based on the detected sequence polymorphisms in GSTs, we hypothesized that contrasting haplotypes would differ in antioxidant response and more specifically in dehydroascorbate reductase (DHAR) activity, which had previously been described as one possible function of GSTs (Edwards and Dixon 2005; Marrs 1996). Contrasting haplotypes did not differ significantly in foliar AsA concentration, but a significant treatment by haplotype interaction was observed in AsA redox state (Table 1): while the tolerant haplotypes had a more oxidized AsA pool under control conditions, the opposite was seen under Fe toxicity. Significant haplotype differences in AsA redox state were consistent with differential DHAR activity, which was significantly up-regulated under Fe stress and significantly lower in the tolerant haplotypes. Total glutathione concentration, MDHAR activity, and glutathione reductase activity were significantly up-regulated under Fe stress, but no significant haplotype effects were detected. In summary, our analyses demonstrated that differences between lines representing the tolerant and sensitive haplotype occurred mostly in DHAR activity and AsA redox state.

Discussion

With 329 different rice accessions from all subpopulations of *O. sativa*, our study represents an extensive screening for tolerance to Fe toxicity in rice and demonstrates considerable variability in tolerance. We considered leaf symptom formation as a relevant phenotype related to Fe tolerance, similar to a number of screening and bi-parental QTL mapping studies reported previously (Dufey et al. 2009, 2012, 2015; Wu et al. 2014), as LBS was demonstrated to be highly correlated with yield formation under Fe-toxic field conditions (Audebert and Fofana 2009). Tolerance rankings reported in different studies sometimes produced contradictory results, presumably due to differences in environmental conditions (e.g., vapor pressure deficit, growth medium), as well as the timing and the intensity of Fe stress (Wu et al. 2014). The tolerance ranking and associated loci presented in this study refer to an acute Fe stress during the vegetative growth stage, as it typically occurs in inland valleys receiving Fe-rich runoff water from adjacent slopes (Becker and Asch 2005). Which tolerance mechanism was dominant under these circumstances: Fe exclusion at the

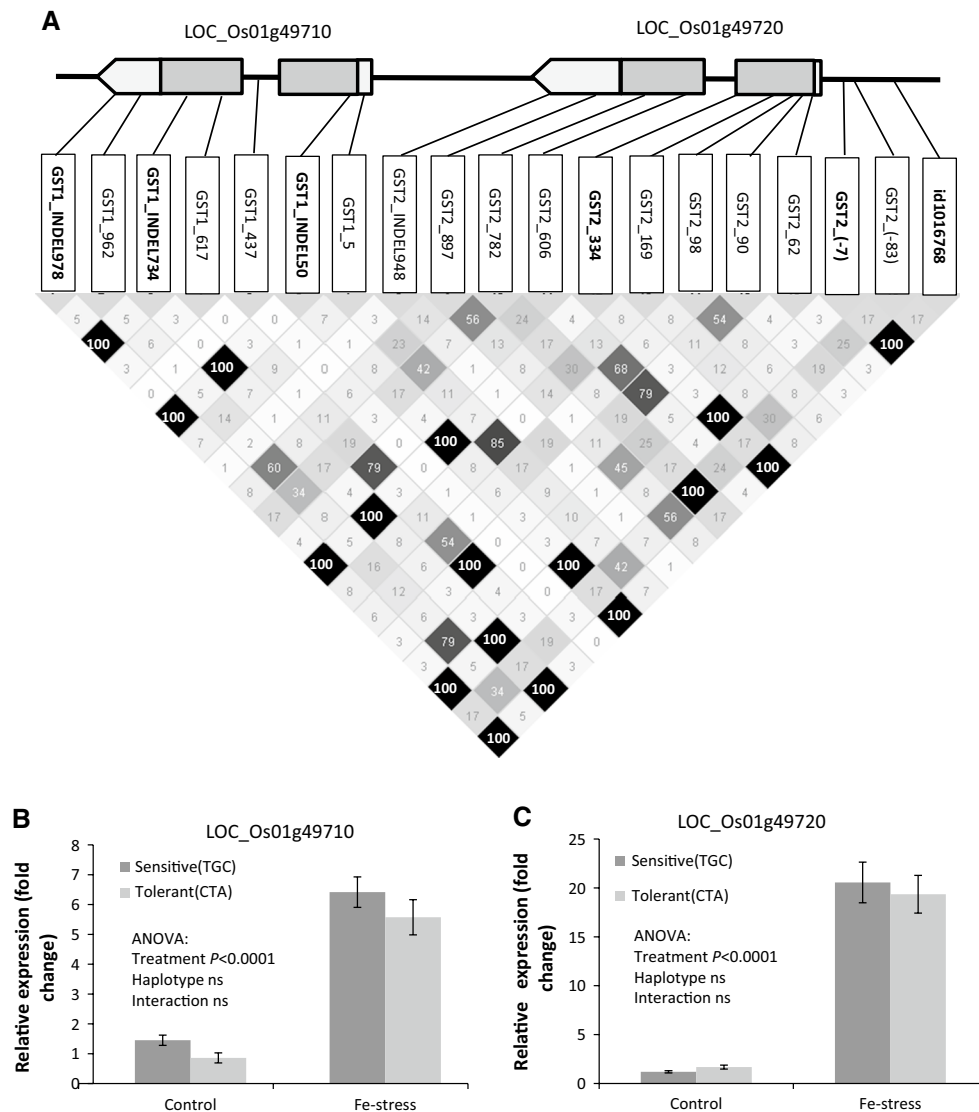


Fig. 4 Sequence and expression analyses of candidate genes LOC_Os01g49710 and LOC_Os01g49720 putatively encoding glutathione-S-transferases. **a** Genomic sequences of 30 representative accessions were aligned. The polymorphisms shown in framed vertical boxes represent SNPs unless the acronym includes ‘INDEL’, in which case they represent an insertion or deletion. The number following the acronym represents the position of the polymorphisms in the MSU7 Nipponbare reference genome counting from the transcript initiation

root surface, or rather shoot-based mechanisms conferring tolerance despite high Fe uptake? Our results suggest that both mechanisms play a role: the correlation between shoot Fe concentration and LBS was significantly positive ($-\log_{10} P > 4.0$, Fig. 1a), suggesting that high Fe uptake was indeed a factor contributing to the formation of visible stress symptoms. However, the linear regression model explained only 15.5 % of the phenotypic variation in LBS, leaving 84.5 % of the variation unexplained by foliar Fe concentrations. That both tolerance mechanisms play a role

site. The triangular matrix indicates linkage disequilibrium ($r^2 \times 100$) between polymorphic sites and the nearby SNP marker id1016768, which had the most significant P value for tLBS5. **(b, c)** Quantitative mRNA expression of LOC_Os01g49710 and LOC_Os01g49720 in contrasting haplotypes under control and Fe-toxic conditions. Haplotypes were defined as in Fig. 2e. Three representative lines per haplotype were analyzed with three experimental replicates in both treatments ($N = 36$)

under acute Fe stress in the vegetative stage is in agreement with our previous study (Wu et al. 2014), which identified QTL associated with both exclusion and inclusion mechanisms in bi-parental populations.

In the association mapping, we followed an approach based on the analysis of LD blocks surrounding significant SNPs, as previously adopted in an association study on tropospheric ozone stress (Ueda et al. 2015). The resolution of association mapping typically depends on the LD: fast LD decay leads to high resolution of mapping, but

Table 1 Substrates and enzymes of the ascorbate–glutathione cycle in contrasting haplotypes differing in leaf bronzing symptoms after 5 days of exposure to Fe toxicity

Variable	Control		Fe toxicity		ANOVA Pr > F		
	Tolerant (CTA)	Sensitive (TGC)	Tolerant (CTA)	Sensitive (TGC)	Treatment	Haplotype	Interaction
Total AsA ($\mu\text{mol g}^{-1}$ FW)	2.75	2.58	2.54	2.67	0.5595	0.8272	0.1687
Reduced AsA ($\mu\text{mol g}^{-1}$ FW)	1.90	2.10	1.95	1.92	0.6757	0.5981	0.4437
DHA ($\mu\text{mol g}^{-1}$ FW)	0.85	0.48	0.58	0.75	0.9934	0.3835	0.0279
AsA redox state (%)	68	81	78	72	0.8806	0.3616	0.0439
Total glutathione ($\mu\text{mol g}^{-1}$ FW)	0.40	0.35	0.54	0.42	0.0334	0.1007	0.5415
GSH ($\mu\text{mol g}^{-1}$ FW)	0.33	0.29	0.45	0.36	0.0560	0.1891	0.6536
GSSG ($\mu\text{mol g}^{-1}$ FW)	0.06	0.06	0.08	0.06	0.2444	0.0688	0.3701
Glutathione redox state (%)	80	81	82	84	0.4844	0.6919	0.8207
APX activity ($\mu\text{mol mg}^{-1}$ protein min^{-1})	1.04	1.32	1.42	1.99	0.0768	0.1478	0.6106
DHAR activity ($\mu\text{mol mg}^{-1}$ protein min^{-1})	0.12	0.20	0.24	0.29	0.0002	0.0080	0.5426
MDHAR activity (nmol mg^{-1} protein min^{-1})	144	138	101	99	0.0017	0.7178	0.8368
GR activity (nmol mg^{-1} protein min^{-1})	26	28	38	40	<0.0001	0.0549	0.8871

Redox state refers to the percentage of reduced AsA or glutathione. Haplotypes refer to SNPs on chromosome 1 exceeding the significance threshold of $-\log_{10} P > 4.0$ for tLBS5 (id1016591, id1016614, and id1016768). Each haplotype was represented by four accessions: CTA Tchibanga (Gabon), Taichung Native 1 (Taiwan), ZHE 733 (China), Sadu Cho (Korea); TGC Guan-Yin-Tsan (China), Kiang-Chou-Chiu (Taiwan), Ming-Hui (China), RTS4 (Vietnam). Three biological replicates were analyzed per accession and LS means of 12 samples are shown ($N = 48$)

AsA ascorbic acid, DHA dehydroascorbic acid, GSH reduced glutathione, GSSG oxidized glutathione, APX ascorbate peroxidase, DHAR dehydroascorbate reductase, MDHAR monodehydroascorbate reductase, GR glutathione reductase

requires a large number of markers to take advantage of many recombination events (Han and Huang 2013; Huang and Han 2014). For the traits tLBS5 and shoot Fe concentration, which are discussed in detail, the identified candidate regions were characterized by a varying degree of LD decay leading to candidate loci (LD blocks) ranging between 12 and 173 kb, containing between 4 and 36 gene models. In our previous GWAS dealing with ozone tolerance, even higher variability in the size of candidate regions was observed, ranging from less than 1 kb to more than 1 Mb. Thus, we assume that using a fixed window approach for declaration of candidate loci (Guo et al. 2009) would be more susceptible to declaring false positive or false negative candidate genes than the approach based on LD blocks.

The analysis of candidate genes was based on annotated genes, although we cannot exclude the possibility of a non-annotated gene being responsible for the phenotype. The candidate LD blocks surrounding highly significant ($-\log_{10} P > 4.0$) SNPs contained various genes with possible involvement in Fe-homeostasis based on their MSU7 annotations (Kawahara et al. 2013). A putative vacuolar ATP-synthase (LOC_Os05g01560) localized within the candidate locus for tLBS5 on chromosome 5 (Fig. 2) could be involved in Fe transport or subcellular Fe partitioning. Vacuolar ATP synthases are membrane localized proteins, which pump protons (H^+) across membranes to generate a

charge gradient for the transport of ions across membranes (Finbow and Harrison 1997). The transport into storage compartments, such as the vacuole, represents an important mechanism for the sequestration of excess ions in plants including Fe (Becana et al. 1998; Schroeder et al. 2013).

The candidate genes for shoot Fe concentration included a casein kinase I (LOC_Os02g56560), which was located in the LD block surrounding the significant SNP on chromosome 2 (Fig. 3). Casein kinases are evolutionarily conserved eukaryotic protein kinases with multiple regulatory roles in plant metabolism and development (Lee 2009; Vidal et al. 2010). In rice, a casein kinase I (different from the one we identified) was shown to be involved in lateral root formation (Liu et al. 2003). Our own previous analyses suggested that the density of lateral fine roots was important in determining the capacity of releasing oxygen into the rhizosphere, which is required for Fe oxidation and precipitation at the root surface, and thus represents a Fe exclusion mechanism (Wu et al. 2014).

Regarding candidate genes located in the peak region on chromosome 1 (Fig. 3), a potassium (K^+) channel (LOC_Os01g45990) putatively involved in potassium transport could be involved in Fe tolerance. Previous studies had shown that K^+ availability mitigated toxic effects of Fe on rice plants by limiting the translocation from roots to shoots (Li et al. 2001).

Among all identified candidate loci, we studied in more detail the two adjacent regions associated with tLBS5 located at around 28.5 Mb on chromosome 1. This region co-localized with several previously reported QTL reported from bi-parental QTL mapping experiments (Dufey et al. 2015; Wu et al. 2014), despite the otherwise low degree of co-localization of QTL obtained from different populations and experimental systems. Although the sensitive haplotype at this locus (TGC) is relatively rare in the association panel (Fig. 2e), it is represented in widely grown mega-varieties such as IR64, which provides scope for adaptive breeding through replacement with the tolerant alleles. The significant SNPs of this region were localized in two LD blocks, both of which contained genes putatively involved in detoxification and redox homeostasis. One was an arabino-lactone oxidase domain containing protein (LOC_Os01g49360) located in the first LD block. This class of enzymes has been shown to be involved in AsA biosynthesis (Smirnov et al. 2001). However, since we did not observe significant differences in total AsA concentrations between contrasting haplotypes for significant SNPs on chromosome 1 (Table 1), we rejected the hypothesis of this gene mediating Fe tolerance via AsA biosynthesis. The second LD block of this region contained two GSTs (LOC_Os01g49710 and LOC_Os01g49720), which had previously been listed by Dufey et al. (2015) as 2 out of 31 candidate genes in this chromosomal region, where multiple QTL co-localized. GSTs constitute a large family of proteins with multiple functions, including detoxification of xenobiotic compounds, stress responses, responses to auxins, and signaling (Edwards and Dixon 2005; Laborde 2010; Marrs 1996). Both genes were up-regulated due to Fe toxicity in the eight genotypes investigated (Fig. 4), although they were not listed among the significantly regulated genes in a previously published microarray study (Quinet et al. 2012), in which a single rice genotype (I Kong Pao) had been exposed to Fe stress. However, the transcriptional regulation was not associated with tolerance, since no differences in mRNA expression levels were observed between tolerant and sensitive haplotypes (Fig. 4). In contrast, sequence analyses revealed polymorphisms between tolerant and intolerant haplotypes, which, in the case of LOC_Os01g49710, caused substantial modifications in the predicted protein structure. Because GSTs were suggested to be involved in oxidative stress response (Edwards and Dixon 2005), we tested the activity of the ascorbate–glutathione cycle in contrasting haplotypes, which constitutes a major component of the plants' ROS detoxification machinery (Noctor and Foyer 1998). Haplotype differences were most pronounced in DHAR activity (Table 1), which constitutes one of the potential functions of plant GSTs (Edwards and Dixon 2005). That lower DHAR activity was associated with tolerance seems counter-intuitive, since high antioxidant activity is typically expected

to confer tolerance to environmental stresses. In the case of this enzyme restoring the reduced form of ascorbate from dehydroascorbate (Noctor and Foyer 1998), it must be considered that reduced ascorbate may not only scavenge ROS, but also reduce Fe^{3+} to Fe^{2+} —a reaction, which is used in widely adopted ascorbate analyses assays (Gillespie and Ainsworth 2007; Ueda et al. 2013). Consequently, the presence of Fe^{2+} may stimulate the Fenton reaction leading to the production of the hydroxyl radical, which cannot be scavenged effectively in plant cells (Apel and Hirt 2004). Thus, in the case of Fe toxicity, the presence of reduced AsA may have a detrimental rather than a protective effect. Based on the above converging evidence, the two GSTs are emerging as plausible candidate genes, which need to be further characterized to address the following questions: (i) whether their involvement in tolerance to Fe toxicity can be confirmed using reverse genetic approaches, and (ii) whether they directly have DHAR activity, or modulate DHAR activity indirectly, e.g., via signaling.

Conclusions

Screening of 329 accessions representing the entire genetic diversity of rice demonstrated that both exclusion and inclusion mechanisms are relevant under an acute short-term Fe stress. GWAS detected multiple loci associated with Fe toxicity tolerance, some of which co-localized with QTL identified previously using bi-parental mapping populations. For these results to make an impact on adaptive rice breeding, the following points need to be considered. (i) The screening protocol aimed at simulating an acute Fe stress during the vegetative growth stage. In the field, Fe toxicity may occur during different growth stages in a barely predictable manner, depending on variable environmental factors such as rainfall. Given the inconsistencies often observed between screening experiments for Fe toxicity tolerance in different environments, further analyses should focus on loci that have repeatedly been reported under different environmental conditions, such as the locus at 28–29 Mb on chromosome 1. Further testing of selected genotypes in different Fe toxic environments may also increase the level of confidence for the selection of suitable donors and traits for breeding. (ii) The loci identified in this study will only be useful for improvement of widely grown cultivars if these carry sensitive alleles at the proposed loci. Further analyses of allelic variants in widely grown mega-varieties are therefore warranted. (iii) The candidate genes nominated in this study need to be verified and functionally characterized in isogenic background. Reverse genetic studies are therefore warranted. Together, these efforts will contribute to the breeding of more adapted cultivars and a better understanding of Fe toxicity tolerance mechanisms in rice.

Author contribution statement EM, LBW, MB, and MF planned the experiment; EM, LBW, YU, SH, and MF conducted the GWAS experiment; EM, LBW, and MF conducted the bioinformatics analyses; LBW and EM conducted the hypothesis testing experiment; LBW, MB, and MF wrote the manuscript.

Acknowledgments This study was financially supported by the *fiat panis* Foundation and Deutsche Forschungsgemeinschaft (DFG, Project ID FR2952-1/1). The authors also wish to thank IRRI for providing seeds and the members of the GRiSP Global Rice Phenotyping Network for sharing experiences in phenotyping and association mapping. We highly appreciate the contributions of many volunteers during the plant phenotyping.

Conflict of interest The authors declare that they have no conflict of interest.

References

- Apel K, Hirt H (2004) Reactive oxygen species: metabolism, oxidative stress, and signal transduction. *Annu Rev Plant Biol* 55:373–399
- Arosio P, Ingrassia R, Cavadini P (2009) Ferritins: a family of molecules for iron storage, antioxidation and more. *Biochim Biophys Acta-Gen Subj* 1790:589–599
- Audebert A, Fofana M (2009) Rice yield gap due to iron toxicity in West Africa. *J Agron Crop Sci* 195:66–76
- Barrett JC, Fry B, Maller J, Daly MJ (2005) Haploview: analysis and visualization of LD and haplotype maps. *Bioinformatics* 21:263–265
- Bashir K, Ishimaru Y, Nishizawa NK (2010) Iron uptake and loading into rice grains. *Rice* 3:122–130
- Becana M, Moran JF, Iturbe-Ormaetxe I (1998) Iron-dependent oxygen free radical generation in plants subjected to environmental stress: toxicity and antioxidant protection. *Plant Soil* 201:137–147
- Becker M, Asch F (2005) Iron toxicity in rice—conditions and management concepts. *J Plant Nutr Soil Sc* 168:558–573
- Blokhina O, Virolainen E, Fagerstedt KV (2003) Antioxidants, oxidative damage and oxygen deprivation stress: a review. *Ann Bot* 91:179–194
- Bradbury PJ, Zhang Z, Kroon DE, Casstevens TM, Ramdoss Y, Buckler ES (2007) TASSEL: software for association mapping of complex traits in diverse samples. *Bioinformatics* 23:2633–2635
- Bradford MM (1976) rapid and sensitive method for quantification of microgram quantities of protein utilizing principle of protein-dye binding. *Analytical Biochem* 72:248–254
- Chen W, Gao Y, Xie W, Gong L, Lu K, Wang W, Li Y, Liu X, Zhang H, Dong H, Zhang W, Zhang L, Yu S, Wang G, Lian X, Luo J (2014) Genome-wide association analyses provide genetic and biochemical insights into natural variation in rice metabolism. *Nature Genet* 46:714–721
- Dobermann A, Fairhurst T (2000) Rice—nutrient disorders and nutrient management. Potash & Phosphate Institute (PPI), Potash and Phosphate Institute of Canada (PPIC) and International Rice Research Institute (IRRI)
- Dufey I, Hakizimana P, Draye X, Lutts S, Bertin P (2009) QTL mapping for biomass and physiological parameters linked to resistance mechanisms to ferrous iron toxicity in rice. *Euphytica* 167:143–160
- Dufey I, Hiel MP, Hakizimana P, Draye X, Lutts S, Kone B, Drame KN, Konate KA, Sie M, Bertin P (2012) Multi-environment quantitative trait loci mapping and consistency across environments of resistance mechanisms to ferrous iron toxicity in rice. *Crop Sci* 52:539–550
- Dufey I, Mathieu A-S, Draye X, Lutts S, Bertin P (2015) Construction of an integrated map through comparative studies allows the identification of candidate regions for resistance to ferrous iron toxicity in rice. *Euphytica* 203:59–69
- Edwards R, Dixon DP (2005) Plant glutathione transferases. In: Helmut S, Lester P (eds) *Methods in Enzymology*. Academic Press, pp 169–186
- Engel K, Asch F, Becker M (2012) Classification of rice genotypes based on their mechanisms of adaptation to iron toxicity. *J Plant Nutr Soil Sc* 175:871–881
- Finbow ME, Harrison MA (1997) The vacuolar H⁺-ATPase: a universal proton pump of eukaryotes. *Biochem J* 324:697–712
- Flint-Garcia SA, Thornsberry JM, Buckler ES (2003) Structure of linkage disequilibrium in plants. *Annu Rev Plant Biol* 54:357–374
- Frei M, Tanaka JP, Chen CP, Wissuwa M (2010) Mechanisms of ozone tolerance in rice: characterization of two QTLs affecting leaf bronzing by gene expression profiling and biochemical analyses. *J Exp Bot* 61:1405–1417
- Frei M, Wissuwa M, Pariasca-Tanaka J, Chen CP, Suedekum K-H, Kohno Y (2012) Leaf ascorbic acid level—is it really important for ozone tolerance in rice? *Plant Physiol Biochem* 59:63–70
- Gabriel SB, Schaffner SF, Nguyen H, Moore JM, Roy J, Blumenstiel B, Higgins J, DeFelice M, Lochner A, Faggart M, Liu-Cordero SN, Rotimi C, Adeyemo A, Cooper R, Ward R, Lander ES, Daly MJ, Altshuler D (2002) The structure of haplotype blocks in the human genome. *Science* 296:2225–2229
- Gillespie KM, Ainsworth EA (2007) Measurement of reduced, oxidized and total ascorbate content in plants. *Nat Protoc* 2:871–874
- Griffith OW (1980) Determination of glutathione and glutathione disulfide using glutathione reductase and 2-vinylpyridine. *Anal Biochem* 106:207–212
- Guo YF, Li J, Bonham AJ, Wang YP, Deng HW (2009) Gains in power for exhaustive analyses of haplotypes using variable-sized sliding window strategy: a comparison of association-mapping strategies. *Eur J Hum Genet* 17:785–792
- Han B, Huang X (2013) Sequencing-based genome-wide association study in rice. *Curr Opin Plant Biol* 16:133–138
- Höller S, Hajirezaei MR, von Wiren N, Frei M (2014) Ascorbate metabolism in rice genotypes differing in zinc efficiency. *Planta* 239:367–379
- Hossain MA, Asada K (1984) Purification of dehydroascorbate reductase from spinach and its characterization as a thiol enzyme. *Plant Cell Physiol* 25:85–92
- Huang X, Han B (2014) Natural variations and genome-wide association studies in crop plants. *Annu Rev Plant Biol* 65:531–551
- Kawahara Y, de la Bastide M, Hamilton JP, Kanamori H, McCombie WR, Ouyang S, Schwartz DC, Tanaka T, Wu J, Zhou S, Childs KL, Davidson RM, Lin H, Quesada-Ocampo L, Vaillancourt B, Sakai H, Lee SS, Kim J, Numa H, Itoh T, Buell CR, Matsumoto T (2013) Improvement of the *Oryza sativa* Nipponbare reference genome using next generation sequence and optical map data. *Rice* 6:4
- Kumagai M, Kim J, Itoh R, Itoh T (2013) Tasuke: a web-based visualization program for large-scale resequencing data. *Bioinformatics* 29:1806–1808
- Laborde E (2010) Glutathione transferases as mediators of signaling pathways involved in cell proliferation and cell death. *Cell Death Differ* 17:1373–1380
- Lee J-Y (2009) Versatile casein kinase 1: multiple locations and functions. *Plant Signal Behav* 4:652–654

- Li H, Yang X, Luo A (2001) Ameniorating effect of potassium on iron toxicity in hybrid rice. *J Plant Nutr* 24:1849–1860
- Liu W, Xu ZH, Luo D, Xue HW (2003) Roles of OsCKII, a rice casein kinase I, in root development and plant hormone sensitivity. *Plant J* 36:189–202
- Marrs KA (1996) The functions and regulation of glutathione S-transferases in plants. *Annu Rev Plant Phys* 47:127–158
- Moore KL, Chen Y, van de Meene AML, Hughes L, Liu W, Geraki T, Mosselmans F, McGrath SP, Grovenor C, Zhao F-J (2014) Combined NanoSIMS and synchrotron X-ray fluorescence reveal distinct cellular and subcellular distribution patterns of trace elements in rice tissues. *New Phytol* 201:104–115
- Noctor G, Foyer CH (1998) Ascorbate and glutathione: keeping active oxygen under control. *Annu Rev Plant Phys* 49:249–279
- Quinet M, Vromman D, Clippe A, Bertin P, Lequeux H, Dufey I, Lutts S, Lefevre I (2012) Combined transcriptomic and physiological approaches reveal strong differences between short- and long-term response of rice (*Oryza sativa*) to iron toxicity. *Plant Cell Environ* 35:1837–1859
- Schroeder JI, Delhaize E, Frommer WB, Guerinot ML, Harrison MJ, Herrera-Estrella L, Horie T, Kochian LV, Munns R, Nishizawa NK, Tsay Y-F, Sanders D (2013) Using membrane transporters to improve crops for sustainable food production. *Nature* 497:60–66
- Smirnoff N, Conklin PL, Loewus FA (2001) Biosynthesis of ascorbic acid in plants: a renaissance. *Annu Rev Plant Phys* 52:437–467
- Stein RJ, Ricachenevsky FK, Fett JP (2009) Differential regulation of the two rice ferritin genes (OsFER1 and OsFER2). *Plant Sci* 177:563–569
- Storey JD, Tibshirani R (2003) Statistical significance for genome wide studies. *Proc Natl Acad Sci USA* 100:9440–9445
- Tamura K, Peterson D, Peterson N, Stecher G, Nei M, Kumar S (2011) MEGA5: molecular evolutionary genetics analysis using maximum likelihood, evolutionary distance, and maximum parsimony methods. *Mol Biol Evol* 28:2731–2739
- Ueda Y, Wu L, Frei M (2013) A critical comparison of two high-throughput ascorbate analyses methods for plant samples. *Plant Physiol Biochem* 70:418–423
- Ueda Y, Frimpong F, Qi Y, Matthus E, Wu L, Höller S, Kraska T, Frei M (2015) Genetic dissection of ozone tolerance in rice (*Oryza sativa* L.) by a genome-wide association study. *J Exp Bot* 66:293–306
- Verslues PE, Lasky JR, Juenger TE, Liu T-W, Kumar MN (2014) Genome-wide association mapping combined with reverse genetics identifies new effectors of low water potential-induced proline accumulation in *Arabidopsis*. *Plant Physiol* 164:144–159
- Vidal D, Alvarez-Florez F, Simon E (2010) Casein kinase activity in etiolated *Cucumis sativus* cotyledons. *Plant Biol* 12:134–144
- White PJ, Broadley MR (2009) Biofortification of crops with seven mineral elements often lacking in human diets—iron, zinc, copper, calcium, magnesium, selenium and iodine. *New Phytol* 182:49–84
- Wissuwa M, Kondo K, Fukuda T, Mori A, Rose MT, Pariasca-Tanaka J, Kretzschmar T, Haeefele SM, Rose TJ (2015) Unmasking novel loci for internal phosphorus utilization efficiency in rice germplasm through genome-wide association analysis. *PLOS One* 10(4):e0124215. doi:10.1371/journal.pone.0124215
- Wu L-B, Shhadi M, Gregorio G, Matthus E, Becker M, Frei M (2014) Genetic and physiological analysis of tolerance to acute iron toxicity in rice. *Rice* 7:8
- Yoshida S, Forno DA, Cock JH, Gomez KA (1976) Laboratory manual for physiological studies of rice, 3rd edn. International Rice Research Institute, Manila
- Zhao K, Tung C-W, Eizenga GC, Wright MH, Ali ML, Price AH, Norton GJ, Islam MR, Reynolds A, Mezey J, McClung AM, Bustamante CD, McCouch SR (2011) Genome-wide association mapping reveals a rich genetic architecture of complex traits in *Oryza sativa*. *Nat Commun* 2:467